Applied Mathematical Sciences, Vol. 20, 2026, no. 3, 115 - 129
HIKARI Ltd, www.m-hikari.com
https://doi.org/10.12988/ams.2026.919326

Magnetoconvection Effects on Micropolar Fluid Flow in a Channel: An Analytical Study

Muhammad Hameed

Department of Mathematics, Science & Technology
Embry-Riddle Aeronautical University
1 Aerospace Boulevard
Daytona Beach, FL 32114, USA

Calvin Fritts

Department of Mathematics & Computer Science
University of South Carolina Upstate
Spartanburg, SC 29316, USA

This article is distributed under the Creative Commons by-nc-nd Attribution License.
Copyright © 2026 Hikari Ltd.

Abstract

We present an analytical series solution for steady magnetoconvection of an electrically conducting micropolar fluid in a vertical parallel-plate channel under the Oberbeck-Boussinesq approximation. The fully developed model yields a coupled boundary-value system for the axial velocity, microrotation, induced magnetic field, and temperature. Adomian's decomposition method is applied directly to the coupled second-order formulation, producing compact truncated series that satisfy the wall conditions and make the dependence on the governing nondimensional parameters explicit. The resulting expressions are used to examine how the Hartmann number, coupling number, micropolar parameter, and buoyancy parameter shape the profiles of $V(y)$, $W(y)$, and $H(y)$. The analysis highlights departures from the Newtonian limit as micropolar coupling strengthens, while increasing magnetic effects damp the axial motion and modify magnetic induction.

Keywords: Micropolar fluid, induced magnetic field, channel flow

1 Introduction

The interaction between magnetic fields and fluid motion is of long-standing interest because of its importance in many technological and natural processes. Conventional Newtonian models, however, are not always adequate for complex materials such as polymer solutions, suspensions, or physiological fluids. To account for such media, Eringen's micropolar fluid theory [1,2] extends the classical continuum description by introducing microstructure and independent microrotation, thereby capturing features that standard models fail to represent, especially in the presence of magnetic fields. Here we investigate thermally driven flow acted on by a uniform transverse magnetic field. The analysis is carried out within the Oberbeck–Boussinesq framework, which allows buoyancy and magnetic effects to be included in a tractable form [3,4,5]. The channel walls, held at constant but possibly unequal temperatures, influence velocity, microrotation, temperature, and the induced magnetic field. These dynamics are vital for optimizing processes like nuclear reactor cooling, geothermal energy extraction, and petroleum refining. The governing equations for the micropolar magnetoconvective flow are solved by means of the Adomian Decomposition Method (ADM) [6,7]. Although ADM is frequently applied to nonlinear problems, it is equally convenient for the present linear but coupled system, because it yields rapidly convergent series solutions without introducing artificial perturbation parameters or restrictive assumptions on the constitutive coefficients. In contrast to earlier analyses [4,5] that transform the system into a single higher-order equation, the present approach retains the original coupled structure and leads to more transparent expressions for the velocity, microrotation, and induced magnetic field.

2 Problem Formulation

We examine the steady, fully developed flow of an electrically conducting micropolar fluid within the Oberbeck-Boussinesq approximation. The fluid occupies the region between two vertical, non-conducting plates that are rigid and fixed in place, separated by a distance $2h$. Each plate is taken to be unbounded in the streamwise and spanwise directions. The medium outside the plates is treated as vacuum (free space), and the corresponding flow configuration is illustrated in Fig. 1.

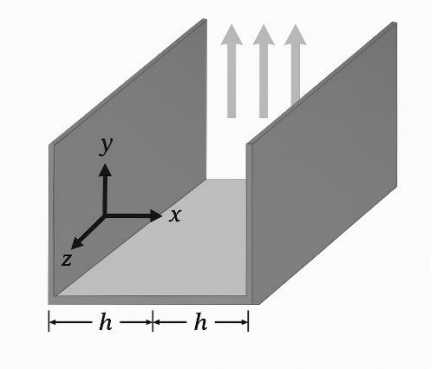

Figure 1: Geometry of the flow

3 Governing Equations

We use the standard incompressible micropolar magnetohydrodynamic model as developed in Eringen's theory [1,2] of micropolar fluids and its subsequent MHD extensions. For an electrically conducting micropolar fluid with constant material properties, the balance laws take the form summarized below.
The continuity equation expresses conservation of mass for an incompressible medium,

$$\boldsymbol{\nabla}.\mathbf{v} = \mathbf{0}, \tag{1}$$

where $\boldsymbol{v}$ is the velocity vector.
The linear–momentum balance, including viscous and microrotational stresses, magnetic body forces and buoyancy, can be written as

$$\begin{aligned}\rho(\mathbf{v}\cdot\boldsymbol{\nabla})\mathbf{v} = -\nabla p + (\mu + \mu_r)\Delta\mathbf{v} + 2\mu_r(\nabla\times\mathbf{w}) \\ + \mu_e(\boldsymbol{\nabla}\times\mathbf{H})\times\mathbf{H} + \rho\alpha_T(T - T_m)\mathbf{g}.\end{aligned} \tag{2}$$

See, for example, Eringen [1] and Borrelli et al. [4,5].
Here $\boldsymbol{p}$ is the pressure, $\mathbf{w}$ is the microrotation vector, $\mathbf{H}$ represents the magnetic field. The parameters μ and μ_r are the classical and micro-rotational viscosities respectively, μ_e is the magnetic permeability, and α_T is the coefficient of thermal expansion. The temperature is denoted T, T_m is a reference temperature, and $\mathbf{g}$ represents the gravitational acceleration.
The angular momentum balance for the microelements leads to the microrotation equation

$$\begin{aligned}\rho j(\boldsymbol{v}\cdot\boldsymbol{\nabla})\mathbf{w} = (c_a + c_d)\Delta\boldsymbol{w} + (c_0 + c_d - c_a)\nabla(\nabla.\mathbf{w}) \\ + 2\mu_r(\boldsymbol{\nabla}\times\mathbf{v} - \mathbf{2w}).\end{aligned} \tag{3}$$

where j is the microinertia and c_a, c_d, c_0 are the spin-viscosity coefficients associated with microrotation. Equation (3) describes the rotational dynamics of the suspended microstructures, incorporating rotational diffusion and coupling with the macroscopic vorticity field.

The magnetic field satisfies the induction equation

$$\eta_e \Delta \boldsymbol{H} = \boldsymbol{\nabla} \times (\boldsymbol{H} \times \mathbf{v}), \tag{4}$$

where η_e is the magnetic diffusivity. The left-hand side represents magnetic diffusion, while the curl of $(\boldsymbol{H} \times \mathbf{v})$ on the right-hand side accounts for convective transport and stretching of magnetic field lines by the flow.

In accordance with Gauss's law for magnetism, the magnetic field is required to be solenoidal (divergence-free), which is expressed mathematically as

$$\boldsymbol{\nabla}.\boldsymbol{H} = \mathbf{0}. \tag{5}$$

This condition enforces the continuity of magnetic field lines.
Finally, the energy equation describing the transport of heat in the fluid is:

$$\boldsymbol{v} \cdot \nabla T = \kappa_t \nabla^2 T, \tag{6}$$

where κ_t is the thermal diffusivity. The left-hand side represents convective changes in temperature, while the right-hand side accounts for thermal diffusion due to conduction.

4 Simple Model Equations

To obtain a tractable model, we restrict attention to a planar, fully developed base flow. The velocity, microrotation, magnetic field, and temperature are assumed to depend only on the transverse coordinate y according to

$$\mathbf{v} = v_1(y)\,\mathbf{e}_1, \qquad \mathbf{w} = w_3(y)\,\mathbf{e}_3, \qquad \mathbf{H} = H_0\mathbf{e}_2 + H_1(y)\,\mathbf{e}_1, \qquad T = T(y),$$

where $\{\mathbf{e}_1, \mathbf{e}_2, \mathbf{e}_3\}$ is the Cartesian basis and $y \in [-h, h]$ measures the distance across the channel. With this ansatz the divergence-free conditions for both $\mathbf{v}$ and $\mathbf{H}$ are automatically satisfied.
Since the flow is unidirectional, $v_1 = v_1(y)$, the convective term $(\mathbf{v} \cdot \nabla)\mathbf{v}$ in the momentum equation vanishes and the pressure becomes a function of x only. Substituting the above forms into the governing equations (1)-(6), and imposing no-slip, no-spin, electrically insulating walls held at fixed temperatures at $y = \pm h$, reduces the partial differential system to a set of coupled second order ordinary differential equations for v_1, w_3, H_1, and T (the intermediate algebra is standard and is omitted here; see, for example, [4,5]).
We now introduce nondimensional variables by scaling the transverse coordinate with the half-width h and using characteristic scales for velocity, microrotation, magnetic field, and temperature. Let

$$y = \frac{x_2}{h}, \qquad V(y) = \frac{v_1(hy)}{V_0}, \qquad W(y) = \frac{h\, w_3(hy)}{V_0},$$

$$H(y) = \frac{H_1(hy)}{V_0\sqrt{\sigma_e \mu_e}}, \qquad \theta(y) = \frac{T(hy) - T_m}{\Delta T},$$

where V_0 is a reference velocity, $T_m = (T_1 + T_2)/2$ is a mean wall temperature, and $\Delta T = T_2 - T_1$ is the imposed temperature difference.
The nondimensional governing equations take the form

$$\frac{d^2V}{dy^2} + 2N^2\frac{dW}{dy} + M(1-N^2)\frac{dH}{dy} + \lambda\,\theta + (1-N^2) = 0, \tag{8a}$$

$$\frac{d^2W}{dy^2} - \frac{M_p^2}{2(1-N^2)}\frac{dV}{dy} - \frac{M_p^2}{1-N^2}\,W = 0, \tag{8b}$$

$$\frac{d^2H}{dy^2} + M\,\frac{dV}{dy} = 0, \tag{8c}$$

$$\frac{d^2\theta}{dy^2} = 0, \tag{8d}$$

subject to $V(\pm 1) = 0,\ W(\pm 1) = 0,\ H(\pm 1) = 0,\ \theta(\pm 1) = \pm\frac{1}{2}.$ (8e)

The parameters N, M_p, M, and λ appearing in (8a)-(8d) are the key dimensionless groups that govern the flow. The coupling number N, or spin-viscosity ratio, is defined by

$$N^2 = \frac{\mu_r}{\mu + \mu_r}, 0 < N^2 < 1,$$

so that $1 - N^2 = \mu/(\mu + \mu_r)$; larger values of N correspond to stronger micropolar (spin) effects.
The micropolar parameter is given by

$$M_p^2 = N^2 l^2, \qquad \text{where } l^2 = \frac{c_d + c_a}{4\mu},$$

which quantifies the coupling between microrotation and the shear field through the spin-viscosity coefficients c_a and c_d; it is inversely related to the characteristic size of the suspended microelements.
The magnetic interaction parameter (Hartmann Number) is given by

$$M^2 = \frac{\sigma_e H_0^2 h^2}{\mu + \mu_r},$$

with σ_e the electrical conductivity and H_0 the imposed transverse magnetic field; in (8a)-(8c) we write M for convenience. Finally, the buoyancy or thermal convection parameter is

$$\lambda = \frac{\mathrm{Gr}}{\mathrm{Re}^2}, \qquad \mathrm{Gr} = \frac{g\,\alpha_T\,\Delta T\,h^3}{\nu^2}, \qquad \mathrm{Re} = \frac{V_0 h}{\nu},$$

where $\nu = (\mu + \mu_r)/\rho$ is the kinematic viscosity, g is the gravitational acceleration, and α_T is the coefficient of thermal expansion. Taken together, these parameters govern the interplay between linear momentum, angular momentum, magnetic induction, and thermal buoyancy in the magnetoconvective micropolar flow described by (8a)–(8e).

Having cast the governing equations into the nondimensional form, we now turn to their analytical solution. Our aim is to construct series representations for $V(y)$, $W(y)$, and $H(y)$ that capture the essential features of the velocity, microrotation, and induced magnetic field throughout the channel, and that make the dependence on the parameters N, M_p, M, and λ completely explicit.

The same boundary-value problem, in essentially the form of (8), has been examined previously in [5], where the coupled system was converted into a single fourth-order ordinary differential equation for the microrotation field and solved by standard methods. While mathematically sound, that procedure requires a lengthy sequence of substitutions and differentiations and tends to obscure the physical coupling among V, W, and H. In the present work we instead apply Adomian's Decomposition Method (ADM) [6] directly to the original set of three second-order differential equations. ADM generates rapidly convergent series [7] by recursively constructing the solution components, without first collapsing the system to a higher-order scalar equation. This strategy preserves the natural coupling between the flow, microrotation, and magnetic field, facilitates the imposition of boundary conditions, and is easily extendable to more general or weakly nonlinear variants of the problem.

5 Adomian Decomposition Method

In preparation for the ADM analysis, we first isolate the temperature equation (8d), which is decoupled from the remaining variables. Integrating this equation subject to the boundary conditions yields the simple linear profile $\theta(y) = y/2$. Substituting this expression into the momentum equation (8a) removes θ from the system and reduces the problem to three coupled equations for $V(y)$, $W(y)$, and $H(y)$.

$$\frac{d^2V}{dy^2} + 2N^2\frac{dW}{dy} + M(1-N^2)\frac{dH}{dy} + \lambda\frac{y}{2} + (1-N^2) = 0, \tag{9a}$$

$$\frac{d^2W}{dy^2} - \frac{M_p^2}{2(1-N^2)}\frac{dV}{dy} - \frac{M_p^2}{1-N^2}\,W = 0, \tag{9b}$$

$$\frac{d^2H}{dy^2} + M\,\frac{dV}{dy} = 0, \tag{9c}$$

In this reduced form the interaction between the velocity, microrotation, and induced magnetic field can be examined more transparently. We then apply the Adomian decomposition method, which is particularly well suited for such coupled systems, and rewrite the governing equations in operator form as follows.

To advance the solution procedure, we act on equations (9a)-(9c) with the inverse

of the second-derivative operator. Denote

$$L^2 = \frac{d^2}{dy^2}$$

and define its inverse L^{-2} by the double integral

$$L^{-2}\{\phi\}(y) = \int_{-1}^{y}\int_{-1}^{s} \phi(t)\, dt\, ds.$$

Applying L^{-2} to each of the equations provides integral representations for V, W, and H. As an illustration, consider (9a). We obtain

$$L^{-2}[L^2V](y) = \int_{-1}^{y}\int_{-1}^{s} V''(t)\, dt\, ds = V(y) - V(-1) - V'(-1)(y+1).$$

Using the boundary condition $V(-1) = 0$ and denoting $V'(-1) = A$, this expression simplifies to

$$L^{-2}[L^2V](y) = V(y) - A(y+1).$$

From the computation above it follows that the action of L^{-2} on L^2V reproduces $V(y)$ itself, apart from a linear term proportional to the boundary derivative at $y = -1$. Because the lower integration limit in the definition of L^{-2} is fixed at -1, the condition $V(-1) = 0$ is automatically incorporated, while the second condition $V(1) = 0$ is used to determine the constant $A = V'(-1)$. In this way both boundary conditions for V are satisfied.

Repeating the same calculation for (9b) and (9c) yields

$$L^{-2}[L^2W](y) = W(y) - B(y+1),$$
$$L^{-2}[L^2H](y) = H(y) - C(y+1),$$

where $B = W'(-1)$ and $C = H'(-1)$ are constants playing roles analogous to A, to be fixed from the boundary conditions for W and H at $y = 1$.

Casting the system of second-order ODEs into these integral forms is a key step in the implementation of the Adomian Decomposition Method, since it allows successive approximations to be constructed while the boundary data are enforced automatically. To make algebra simple and for later convenience we introduce, $\Delta = 1 - N^2$.

The system (9a)–(9c) can be rewritten in the form

$$V(y) = -L^{-2}\left\{2N^2W'(y) + M\Delta\, H'(y) + \frac{\lambda}{2}y + \Delta\right\} + A\,(y+1),$$
$$W(y) = L^{-2}\left\{\frac{M_p^2}{2\Delta}\, V'(y) + \frac{M_p^2}{\Delta}\, W(y)\right\} + B\,(y+1),$$
$$H(y) = -L^{-2}\{MV'(y)\} + C\,(y+1).$$

These integral representations provide the starting point for constructing the ADM series for V, W, and H.

In the Adomian framework, the unknown fields are expanded as

$$V(y) = \sum_{n=0}^{\infty} V_n(y), \qquad W(y) = \sum_{n=0}^{\infty} W_n(y), \qquad H(y) = \sum_{n=0}^{\infty} H_n(y).$$

The component functions V_n, W_n, H_n are generated successively. In accordance with the homogeneous boundary conditions $V(\pm 1) = W(\pm 1) = H(\pm 1) = 0$, we choose the zeroth–order terms as

$$V_0(y) = 0, \qquad W_0(y) = 0, \qquad H_0(y) = 0.$$

With this choice, and using (9a) together with $W = W_0$ and $H = H_0$, the first nontrivial contribution to the velocity arises from the nonhomogeneous forcing, giving

$$V_1(y) = -L^{-2}\left[\frac{\lambda}{2}y + \Delta\right] + A_1(y+1),$$

where $\Delta = 1 - N^2$. Evaluating the double integral and then employing the conditions $V_1(1) = 0$, which gives $A_1 = \Delta - \frac{\lambda}{6}$.

$$V_1(y) = -\frac{\lambda}{12}(y^3 - y) + \frac{\Delta}{2}(1 - y^2).$$

Because $W_0 = 0$ and $H_0 = 0$, the corresponding first-order corrections vanish,

$$W_1(y) = 0, \qquad H_1(y) = 0.$$

For higher orders ($n \geq 1$), the component functions satisfy the recurrence relations

$$\begin{aligned}
V_{n+1}(y) &= -L^{-2}\{2N^2 W_n'(y) + M\Delta\, H_n'(y)\} + A_{n+1}(y+1),\\
W_{n+1}(y) &= L^{-2}\left\{\frac{M_p^2}{2\Delta}\, V_n'(y) + \frac{M_p^2}{\Delta}\, W_n(y)\right\} + B_{n+1}(y+1),\\
H_{n+1}(y) &= -L^{-2}\{M V_n'(y)\} + C_{n+1}(y+1),
\end{aligned}$$

where the constants A, B, and C are those introduced earlier through the action of L^{-2} and are determined by the boundary conditions for V, W, and H, respectively. At the second order of the decomposition (i.e., for $n = 1$), the relation for V_2 yields trivial contribution $V_2(y) = 0$. The microrotation component W_2, which is driven by the derivative $V_1'(y)$, is obtained as

$$W_2(y) = \frac{M_p^2}{2\Delta}\left[-\frac{\lambda}{48}(y^2 - 1)^2 - \frac{\Delta}{6}(y^3 - y)\right].$$

The corresponding second-order correction to the induced magnetic field, also forced by $V_1'(y)$, takes the form

$$H_2(y) = \frac{M\lambda}{48}(y^2-1)^2 + \frac{M\Delta}{6}(y^3-y).$$

Advancing to the third order we determine $V_3(y)$, $W_3(y)$, and $H_3(y)$. The velocity component $V_3(y)$ incorporates the influence of the coupling through $W_2(y)$ and $H_2'(y)$, and can be written as

$$V_3(y) = -\frac{K}{24}(y^2-1)^2 - \frac{\lambda K}{720\Delta}\, y(y^2-1)(3y^2-7),$$

where $K = \Delta^2 M^2 + M_p^2(\Delta - 1)$.

The third-order microrotation term $W_3(y)$ then follows from the recurrence relation and represents the accumulated effect of the lower-order velocity and magnetic field contributions. A compact factorized form is:

$$W_3(y) = -\frac{M_p^4}{2880\Delta^2}(y^2-1)[12\Delta y^3 - 28\Delta y + \lambda(y^4 - 4y^2 + 11)].$$

At the same order the induced magnetic field does not receive any additional contribution, so that $H_3(y) = 0$.

To account for higher-order iterative corrections, the procedure is continued to the fourth level of the ADM expansion, from which $W_4(y)$ and $H_4(y)$ are obtained by inserting (V_3, W_3, H_3) into the recurrence relations. The resulting expressions are given below:

$$H_4(y) = \frac{M\left(\Delta^2 M^2 + \Delta M_p^2 - M_p^2\right)}{1440\Delta}(y^2-1)[12\Delta y^3 - 28\Delta y + \lambda(y^4 - 4y^2 + 3)].$$

$$W_4(y) = \frac{M_p^2(1-y^2)}{483840\Delta^3}\left[168\Delta K\,\{12\Delta y^3 - 28\Delta y + \lambda(y^4 - 4y^2 + 3)\} + M_p^4 R(y)\right],$$

where $R(y) = 16\Delta\, y(3y^4 - 18y^2 + 31) + \lambda(3y^6 - 25y^4 + 185y^2 - 739)$.

Retaining all nonzero components up to this order, the approximate profiles of velocity, microrotation, and induced magnetic field may be written as the truncated series

$$\begin{aligned}
&\theta(y) = y/2,\\
&V(y) \approx V_1(y) + V_3(y) + \cdots,\\
&W(y) \approx W_2(y) + W_3(y) + W_4(y) + \cdots,\\
&H(y) \approx H_2(y) + H_4(y) + \cdots.
\end{aligned}$$

The truncated ADM representations obtained above provide explicit closed-form

approximations for $V(y)$, $W(y)$, and $H(y)$ throughout the channel, with coefficients that depend transparently on the nondimensional groups N, M, M_p, and λ. In practice, the approximation can be systematically refined by generating additional components from the same recurrence relations, and its quality can be assessed by substituting the truncated series back into the governing system and evaluating the resulting residuals. The present truncation is adopted as a compact analytic benchmark and as a computationally efficient surrogate for direct boundary-value solvers. In the next section, these expressions are used to examine how magnetic damping, micropolar coupling, and buoyancy shape the profiles of the velocity, microrotation, and induced magnetic field.

6 Graphical Results

Figures 2-7 summarize the influence of the key nondimensional parameters on the cross-channel distributions of axial velocity $V(y)$, microrotation $W(y)$, and induced magnetic field $H(y)$ for $y \in [-1,1]$. The coupling number N quantifies the interaction between the macroscopic shear field and particle microrotation; $N \to 0$ recovers the Newtonian MHD limit, whereas larger N corresponds to stronger micropolar coupling. The Hartmann number M measures the strength of the applied magnetic field and therefore the magnitude of Lorentz braking in the momentum balance. The micropolar parameter M_p controls the level of microrotation activity, and the buoyancy parameter λ governs the magnitude and direction of the thermally driven forcing (with the sign of λ distinguishing opposing versus aiding buoyancy).

Figures 2-4 display the axial velocity $V(y)$. In Figure 2, for $\lambda = 0$, the velocity remains symmetric about the centerline and strictly nonnegative for the parameter range shown. Increasing the magnetic field strength (larger M) reduces the velocity magnitude and produces a progressively flatter, more plug-like core, consistent with Lorentz damping. The sensitivity of V to M is strongest at smaller coupling (e.g., $N = 0.2$-0.4), while at larger coupling (e.g., $N = 0.8$) the velocity magnitude is already substantially reduced and the spread between different M values becomes comparatively small. For $\lambda = 2$ (Figure 3), the velocity profile becomes skewed across the channel (peak shifted away from the centerline), while the magnetic damping trend with increasing M remains evident. Figure 4 isolates the role of micropolar coupling at fixed $M = 2$ and $M_p = 1$: the curves for $N = 0$ and $N = 0.2$ are nearly indistinguishable, whereas larger coupling (e.g., $N = 0.6$-0.8) produces a remarkable reduction in $V(y)$ and enhances the profile skewness when $\lambda \neq 0$.

Figure 5 presents microrotation profiles $W(y)$ for representative parameter sets at fixed $M = 2$. Increasing the coupling number N increases the magnitude of microrotation (larger extrema), indicating stronger transfer between translational motion and micro-spin. Increasing M_p also amplifies microrotation substantially, yielding larger $W(y)$ across the channel. Variations in λ strongly affect both the

magnitude and the sign distribution of W: positive λ strengthens the negative lobe of W(more negative minima), whereas negative λ reverses the trend and increases the positive lobe in the channel interior, reflecting the directional change in buoyancy forcing.

Figures 6 and 7 show the induced magnetic field $H(y)$. For fixed $M = 2$, $M_p = 1$, and $N = 0.4$ (Figure 6), increasing $|\lambda|$ increases the amplitude of $H(y)$; moreover, changing the sign of λ significantly alters the balance between positive and negative lobes of H. Figure 7 highlights the distinct roles of micropolar parameters: increasing M_p increases the magnitude of the induced field, whereas increasing the coupling number N reduces the induced-field amplitude over the channel. Taken together, these plots demonstrate that the magnetic field strength M primarily damps the axial motion, while the micropolar parameters N and M_p strongly modulate microrotation and magnetic induction, and λ controls the degree of asymmetry and the directionality of the buoyancy-driven response.

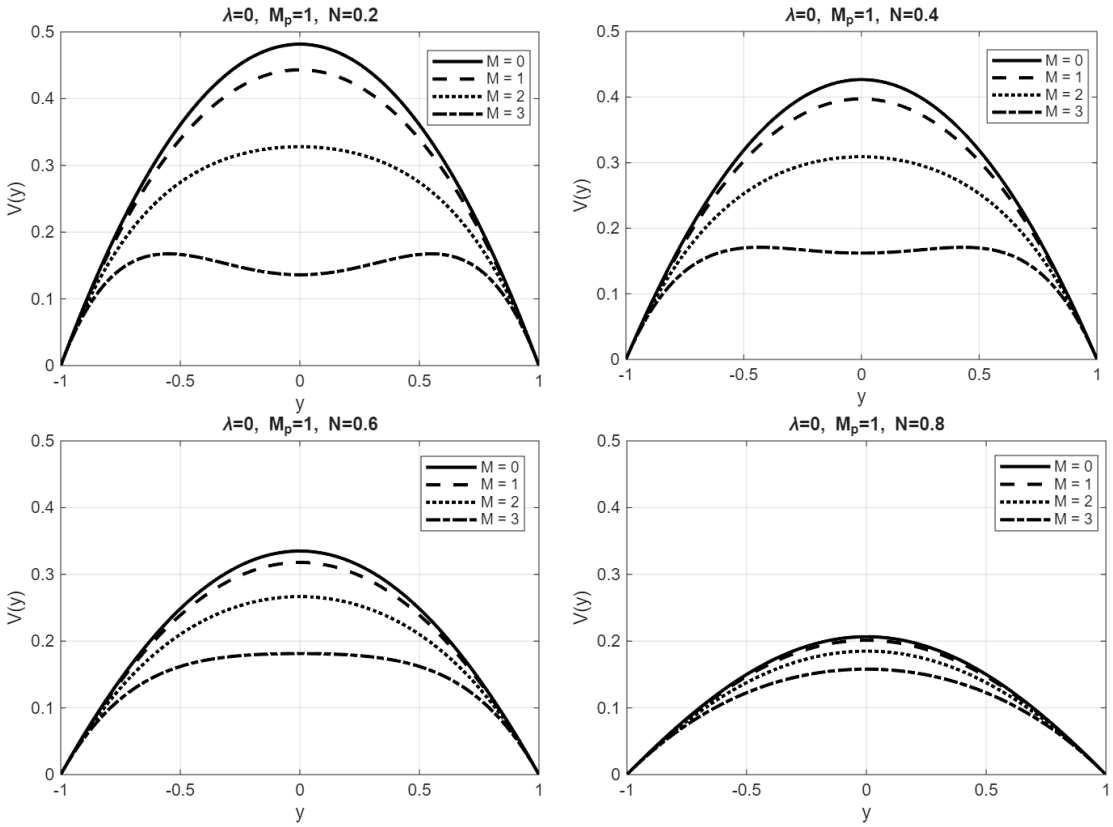

Figure 2 Velocity V for the case of λ = 0. The influence of M on the velocity as the coupling number increases (N = 0.2, 0.4, 0.6, 0.8).

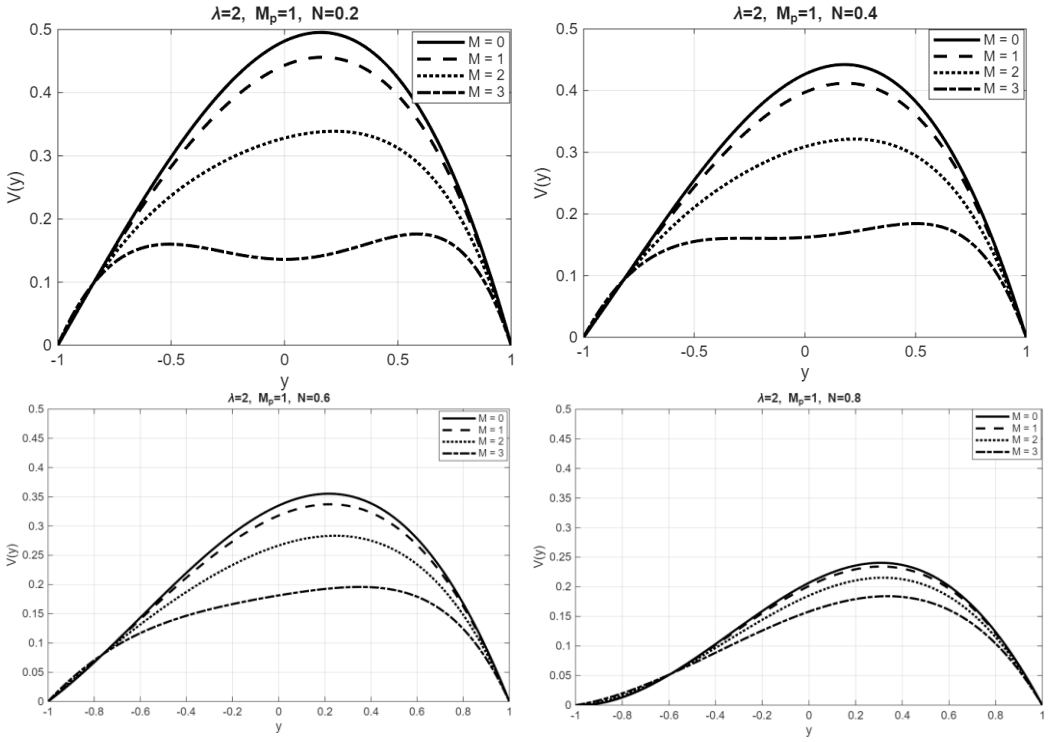

Figure 3: Variation of the velocity profile $V(y)$ for $\lambda = 2$ and $M_p = 1$. The influence of the Hartmann number M is shown for different values of the coupling number $N = 0.2, 0.4, 0.6, 0.8$.

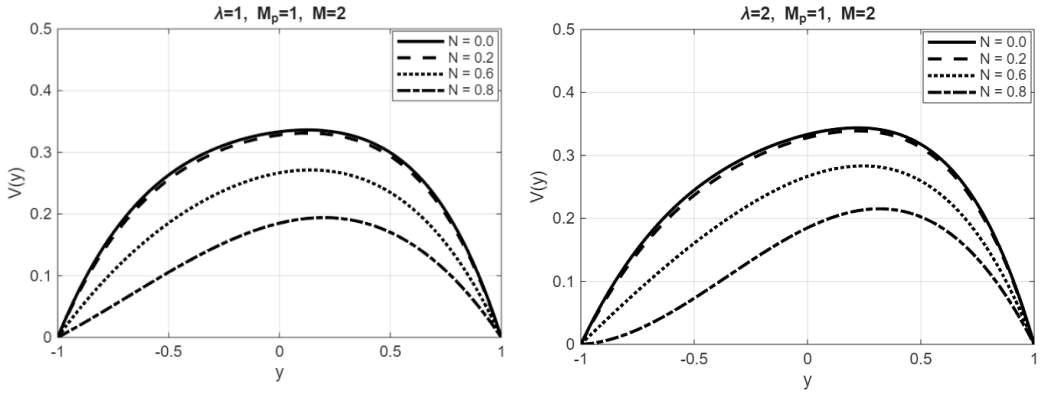

Figure 4: Variation of the velocity profile $V(y)$ with changing thermal convection parameter λ for fixed $M_p = 1$ and $M = 2$. The effect of the coupling parameter N is illustrated for (a) $\lambda = 1$ and (b) $\lambda = 2$.

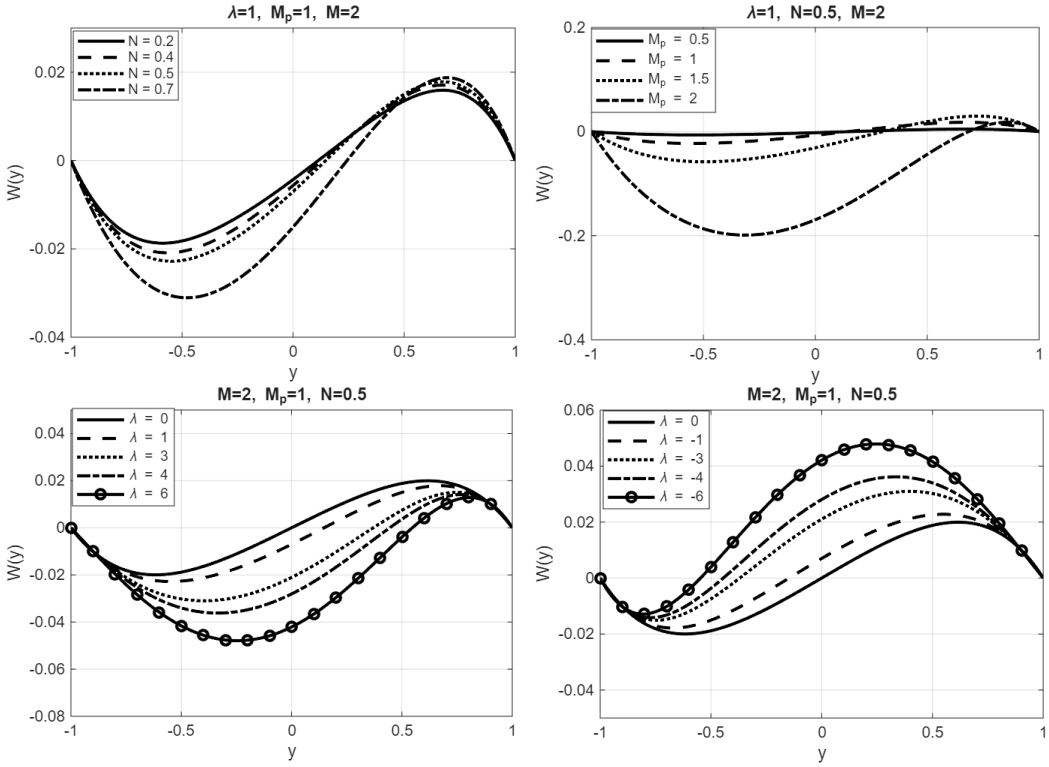

Figure 5: Microrotation profiles $W(y)$ for various parameter combinations with $M = 2$. Top-left: effect of the coupling parameter N for $M_p = 1$ and $\lambda = 1$. Top-right: effect of the microrotation parameter M_p for $N = 0.5$ and $\lambda = 1$. Bottom-left and bottom-right: effect of the buoyancy parameter λ for $M_p = 1$ and $N = 0.5$.

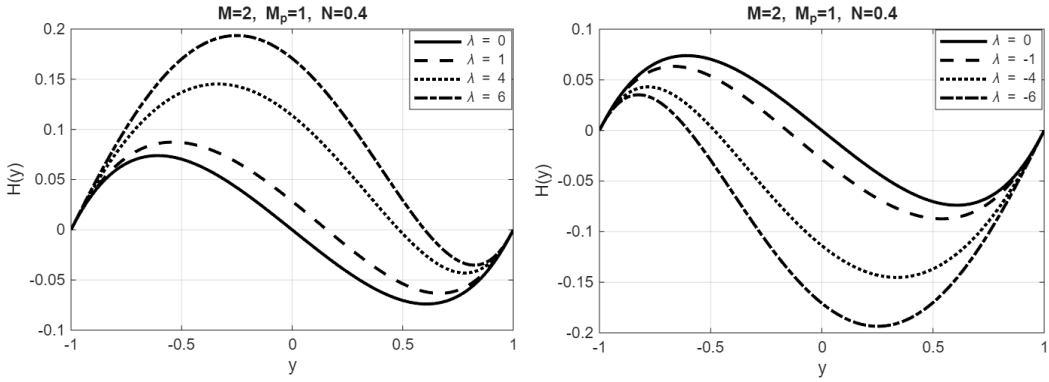

Figure 6: Variation of the induced magnetic field $H(y)$ at $M = 2$, $M_p = 1$, and $N = 0.4$ for different values of the buoyancy parameter λ. The left panel corresponds to positive λ, while the right panel shows negative λ.

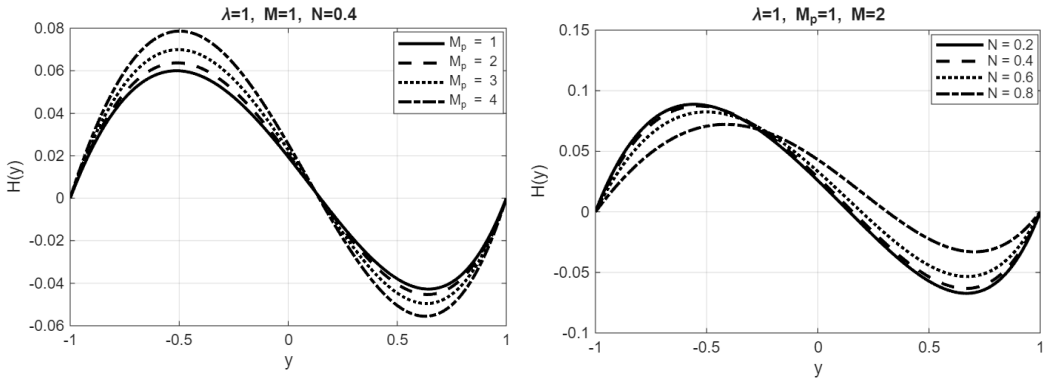

Figure 7: Variation of induced magnetic field $H(y)$ for various parameter combinations. Left: effect of the microrotation parameter M_p for $\lambda = 1$, $M = 1$, and $N = 0.4$. Right: effect of the coupling parameter N for $\lambda = 1$, $M_p = 1$, and $M = 2$.

7 Concluding Remarks

We examined steady magnetoconvective flow of an electrically conducting micropolar fluid in a vertically oriented parallel-plate channel under the Oberbeck-Boussinesq approximation. After nondimensionalization, the governing model reduces to a coupled boundary-value problem for the axial velocity $V(y)$, microrotation $W(y)$, induced magnetic field $H(y)$, and temperature. Using the Adomian Decomposition Method (ADM), we constructed rapidly convergent series representations and obtained explicit truncated expressions that allow direct evaluation of the flow and field profiles over broad parameter ranges. Because ADM was applied directly to the coupled second-order system, the natural coupling among V, W, and H is preserved without transforming the model into a single higher-order equation, and the resulting closed forms provide a convenient basis for parametric investigation.

The graphical results (Figures 2-7) show that magnetic, buoyancy, and micropolar effects interact in a systematic way. The applied magnetic field, represented by the Hartmann number M, acts primarily as a braking mechanism: increasing M reduces the axial velocity magnitude and flattens the velocity profile. The coupling number N has a pronounced micropolar influence; increasing N reduces the axial velocity while increasing the magnitude of microrotation, consistent with stronger transfer between translational shear and micro-spin. The micropolar parameter M_p significantly amplifies microrotation and also strengthens the induced magnetic field. The buoyancy parameter λ controls asymmetry and directionality: $\lambda = 0$ yields symmetric velocity profiles, while $\lambda \neq 0$ produces skewed velocity distributions and strongly modifies both $W(y)$ and $H(y)$. In particular, increasing $|\lambda|$ increases the amplitude of the induced magnetic field, and reversing the sign of λ alters the balance between positive and negative lobes of both W and H, reflecting

the reversal of buoyancy forcing.
Overall, the explicit ADM solutions developed here provide a compact analytical benchmark for micropolar magnetoconvection in channels and facilitate rapid assessment of parameter sensitivity in applications involving electrically conducting complex fluids. The present framework is readily extendable to more general thermal boundary conditions, spatially varying magnetic fields, or time-dependent configurations, and thus provides a flexible starting point for broader micropolar MHD heat-transfer studies.

Acknowledgements. First author gratefully acknowledges financial support from the Dean's Start-up Fund of the College of Arts & Sciences, Embry-Riddle Aeronautical University-Worldwide.

References

[1] A. C. Eringen, Theory of micropolar fluids, *Journal of Mathematics and Mechanics*, **16** (1966), 1-18. https://doi.org/10.1512/iumj.1967.16.16001

[2] A. C. Eringen, *Microcontinuum Field Theories, Vol. I: Foundations and Solids,* Springer, New York, 1999. https://doi.org/10.1007/978-1-4612-0555-5

[3] G. Lukaszewicz, *Micropolar Fluids: Theory and Applications*, Birkhäuser, Basel, 1999.

[4] R. Borrelli, A. Giantesio, and M. C. Patria, Natural convection for incompressible micropolar fluids in the presence of a magnetic field, *Nonlinear Analysis: Real World Applications*, **24** (2015), 26-49.

[5] R. Borrelli, A. Giantesio, and M. C. Patria, Magnetoconvection of a micropolar fluid in a vertical channel, *International Journal of Heat and Mass Transfer*, **80** (2015), 614-625. https://doi.org/10.1016/j.ijheatmasstransfer.2014.09.031

[6] G. Adomian, *Solving Frontier Problems of Physics: The Decomposition Method,* Kluwer Academic Publishers, Dordrecht, 1994. https://doi.org/10.1007/978-94-015-8289-6

[7] G. Adomian, *Nonlinear Stochastic Systems Theory and Applications to Physics*, Kluwer Academic Publishers, Dordrecht, 1989. https://doi.org/10.1007/978-94-009-2569-4

Received: March 11, 2026; Published: April 3, 2026